Assessing the effectiveness of trees for landslide mitigation in Hawke's Bay

Prepared for: Hawke’s Bay Regional Council June 2024

Hawkes Bay Regional Council Publication No. 5660

HAWKES BAY REGIONAL COUNCIL

TE KAUNIHERA Ā-ROHE O TE MATAU-A-MĀUI

ISSN 2703-2051 (Online)
ISSN 2703-2043 (Print)

(06) 835 9200
0800 108 838
Private Bag 6006 Napier 4142
159 Dalton Street . Napier 4110

Environmental Science

Assessing the effectiveness of trees for landslide mitigation in Hawke's Bay

Prepared for: Hawke’s Bay Regional Council June 2024

Hawkes Bay Regional Council Publication No. Report number 5660

Reviewed By:

Dr Ashton Eaves – Senior Land Scientist

Approved By:

Sam French – Science Manager

ISSN 2703-2051 (Online)
ISSN 2703-2043 (Print)

.

Assessing the effectiveness of trees for landslide mitigation in Hawke's Bay

Prepared for: Hawke's Bay Regional Council

June 2024

Assessing the effectiveness of trees for landslide mitigation in Hawke's Bay

Contract Report: LC4479

Anatolii Tsyplenkov, Hugh Smith

Manaaki Whenua – Landcare Research

Reviewed by:	*Approved for release by:*
Andrew Neverman Researcher – Geomorphology Manaaki Whenua – Landcare Research	John Triantafilis Portfolio Leader – Managing Land & Water Manaaki Whenua – Landcare Research

Contents

Summary

Project and client

- Hawke's Bay Regional Council (HBRC) contracted Manaaki Whenua – Landcare Research (MWLR) to assess the effectiveness of individual trees for reducing the occurrence of rainfall-induced shallow landslides on farms in the region.
- As part of this project, HBRC asked MWLR to estimate the magnitude of reductions in the number of shallow landslides and the amount of landslide sediment delivered to streams that might have been achieved by the presence of individual trees in pastoral areas during Cyclone Gabrielle.
- The work on assessing the effectiveness of trees for shallow landslide mitigation was completed under the Extreme Weather Recovery Advice Fund (contract ID C09X2303).

Objectives

The project had the following objectives.

- Model the reduction in the number of rainfall-induced shallow landslides due to the presence of individual trees on pastoral land during Cyclone Gabrielle for 50 farms in the Hawke's Bay region.
- Model the reduction in landslide-derived sediment load delivered to the stream network due to the presence of trees in pasture areas on the selected farms during Cyclone Gabrielle.
- Produce combined shallow landslide susceptibility and connectivity raster maps for the selected farms.

Methods

- The influence of individual trees on farm-scale landslide erosion and sediment loads was modelled for (a) the baseline scenario, whereby existing trees in pastoral areas were removed; (b) the contemporary tree cover scenario. The analysis used a tree map produced for HBRC by MWLR as part of the HBRC–MWLR LiDAR partnership project (2022–2024) and a landslide inventory for Cyclone Gabrielle from the GNS-led mapping project (see Leith et al. 2023).
- The selection of farms for analysis focused on pastoral areas on farms that experienced high rainfall during Cyclone Gabrielle but varied levels of landsliding. The AgriBase data set was used to identify farm boundaries, and the New Zealand Land Cover Database (LCDB v5.0, 2018) was used to retrieve the farm-pasture polygons.
- The existing statistical model representing the influence of individual trees on landslide susceptibility (Spiekermann et al. 2021, 2022a) was updated using available data on individual trees and a LiDAR-derived digital elevation model (DEM) for pastoral areas with landslide scar area data from semi-automated mapping in northern Hawke's Bay by Betts et al. (2023).
- Using the shallow landslide susceptibility and morphometric connectivity model framework from Spiekermann et al. 2022a and Tsyplenkov et al. 2023, we estimated sediment delivery to streams by shallow landslides for the two scenarios.

- The difference in landslide occurrence between the two scenarios was used to estimate the reduction in landslide erosion and sediment delivery to streams associated with the presence of individual trees on pastoral land.

Results

- Cyclone Gabrielle triggered 20,392 shallow landslides across all the selected farms. The corresponding gross shallow landslide erosion was estimated to be 2.54×10^6 t, while an estimated 0.17×10^6 t (6.6%) of landslide-derived sediment reached the stream network.
- With trees removed from pastoral areas, we estimated that 22,257 shallow landslides could have been triggered by Cyclone Gabrielle. That count resulted in gross landslide erosion of 2.77×10^6 t with an estimated 0.18×10^6 t (6.5%) of sediment delivered to the stream network.
- Farm-scale modelling revealed that existing tree cover may have prevented an additional 1,865 landslides occurring (8.4%), or, when expressed as gross landslide erosion, 0.23×10^6 t of eroded material.
- The presence of trees in pastoral areas achieved an estimated median 7% reduction in landslide numbers across the 50 farms. When expressed as sediment yield, this equated to a median 10% decrease in landslide erosion, irrespective of whether sediment was delivered to the stream network.
- The existing tree cover on pastoral land led to an estimated 9% reduction in landslide sediment delivery to streams when summed across all farms. This proportional reduction equates to approximately 16,150 t of sediment that was prevented from reaching the stream network due to the influence of trees in stabilising land and reducing the occurrence of landslides during Cyclone Gabrielle.

Conclusions and recommendations

- Our analysis showed that existing tree cover in pastoral areas prevented an estimated 1,865 additional landslides across all farms, with a median 7% reduction in landslide count. This equates to a median 10% decrease in sediment yield delivered to streams. In areas with trees near streams and on susceptible slopes, sediment delivery reductions of up to 24% were estimated.
- The main driver of the reductions in sediment delivery was tree density in pastoral areas highly susceptible to landslides, where landslide runout was likely to connect with the stream network. This area has already been reduced from 5.7% to 4.7% across all farms due to existing trees.
- Further reductions in future landslide sediment delivery to streams could be achieved through additional tree planting targeting pasture areas that are highly susceptible and highly likely to produce landslides that connect to streams. These areas have been identified in the farm-scale landslide susceptibility and connectivity maps accompanying this report.

1 Introduction

Cyclone Gabrielle triggered a large number of shallow landslides across the Hawke's Bay region, resulting in extensive land damage and substantial sediment deposition in downstream environments. In response to this event, Hawke's Bay Regional Council (HBRC) engaged Manaaki Whenua – Landcare Research (MWLR) to assess the effectiveness of existing trees in reducing the occurrence of rainfall-induced shallow landslides on selected farms in the region.

The present report adopts a data-driven, statistical modelling approach designed to quantify the impact of individual trees in pastoral areas on landslide susceptibility and the spatial probability of landslide-derived sediment reaching streams. The analysis uses a tree map produced for HBRC by MWLR as part of the HBRC–MWLR LiDAR partnership project (2022–2024). The model was applied to farms exhibiting a range of landslide susceptibility, tree cover, and landslide damage from Cyclone Gabrielle, facilitating a comparative assessment of the effectiveness of individual trees in reducing landslides under varying conditions.

The findings from this report will help HBRC to communicate to stakeholders the influence of existing trees in pastoral areas on the incidence of landslides triggered by the cyclone. The insights gained may also help target future tree planting to areas most susceptible to landslides and where landslides are most likely to contribute sediment to streams. This information is crucial for enhancing land management practices and limiting the future occurrence of shallow landslides in the region.

2 Background

Between 12 and 16 February 2023 an extreme rainfall event, referred to as Cyclone Gabrielle, affected much of the northern North Island of New Zealand, causing widespread damage. It was a severe event that required a national-level response. States of emergency were declared for seven regions of New Zealand. Along with surface, coastal, and river flooding, the event triggered more than 140,000 landslides, delivering significant amounts of sediment to downstream receiving environments (Leith et al. 2023).

Recent work by Spiekermann et al. (2022a, 2022b) proposed a data-driven model framework to quantify the effectiveness of trees for mitigating rainfall-induced shallow landslide erosion. The approach is based on coupling a landslide susceptibility model with a morphometric, landslide-to-stream connectivity model. The landslide susceptibility model included high-resolution, spatially explicit representation of the influence of individual trees at the landscape scale.

This model framework provides a basis for estimating reductions in the number of shallow landslides and the amount of landslide sediment delivered to streams that may have been achieved by the presence of trees in pastoral areas on farms in Hawke's Bay during Cyclone Gabrielle.

3 Objectives

The project had three objectives.

- Model the reduction in the number of rainfall-induced shallow landslides due to the presence of individual trees on pastoral land during Cyclone Gabrielle for 50 farms in the Hawke's Bay region.
- Model the reduction in landslide-derived sediment load delivered to the stream network due to the presence of trees in pasture areas during Cyclone Gabrielle on the selected farms.
- Produce combined shallow landslide susceptibility and connectivity raster maps for the selected farms.

4 Methods

Using the shallow landslide susceptibility and connectivity model framework from Spiekermann et al. 2022a and Tsyplenkov et al. 2023, we estimated sediment delivery to streams by shallow landslides for:

- a treeless scenario, where existing individual trees within pastoral areas on the selected farms were removed, called the 'baseline' scenario;
- an existing trees scenario, comprising the contemporary tree cover derived from the 2020/21 regional LiDAR survey, called the 'real' scenario.

We also compared the model's spatial predictions with interim landslide mapping data for Cyclone Gabrielle (data accessed on 1 November 2023) in the Hawke's Bay region (Leith et al. 2023). Our focus was farms that experienced high rainfall during Cyclone Gabrielle but varied levels of landsliding. The difference in landslide occurrence reflects, in part, the presence of trees and landscape susceptibility. Comparing the model results for the two scenarios allowed us to assess the extent to which the presence of individual trees on pastoral land reduced landslide occurrence and sediment delivery to streams.

4.1 Farm selection

Using geospatial information on farm boundaries and pastoral land cover, we selected 50 farms that were susceptible to landslide occurrence where landslide source points were mapped and the maximum 48 h rainfall during Cyclone Gabrielle uniformly exceeded 150 mm across the farm polygon (a typical threshold for landslide triggering; Basher et al. 2020). The selection procedure was as follows.

1. AgriBase (Sanson 2005) farm polygons were intersected with 'pasture' land (i.e. 'low' and 'high' producing grassland classes) from the New Zealand Land Cover Database (LCDB v5.0, 2018). Given the focus on the effectiveness of individual trees in pastoral land, we removed areas on the farm with continuous forest or scrub cover.
2. The resulting farm-pasture polygons from step 1 were filtered based on:

- at least 95% of the farm-pasture polygon area intersected mapping grids containing Cyclone Gabrielle landslide data (from the GNS-led mapping project, see Leith et al. 2023)
- at least 95% of the farm-pasture polygon area received at least 150 mm of rain in 48 h (from the HBRC 48 h rainfall map for Cyclone Gabrielle)
- mean rainfall was ≥250 mm in 48 h per farm-pasture polygon
- the area of discontinuous farm-pasture polygon was ≥1 km^2
- landslide density was ≥10 scars/km^2.

First, we used the AgriBase layer to subset farms into specific classes. Polygons with the 'farm_type' attribute equal to 'MTW', 'NEW', 'OTH', 'SLY', 'URB', 'NAT', 'FOR', 'NOF', 'UNS', 'LIF' were omitted. These polygons represent plantation forests, urban areas and infrastructure, and scrub areas. The subsetted AgriBase layer was then united with the LCDB polygons to create polygons containing both farm-type and land-cover classes. For further analysis, only polygons identified in LCDB as 'High Producing Exotic Grassland' and 'Low Producing Grassland' were selected to represent pastoral areas.

The rainfall threshold of 150 mm in 48 h over >95% of each farm-pasture polygon area was chosen to ensure that most pasture areas on the farm experienced rainfall that exceeded a typical threshold for initial landslide triggering (Basher et al. 2020). The additional criterion of mean rainfall ≥ 250 mm in 48 h allowed us to further subset the polygons to those with higher rainfall that may trigger a higher density of landslides for subsequent analysis. This approach was designed to reduce the chance that a relative lack of landslides on any farm was due to insufficient storm rainfall.

The second constraint on farm selection was the overlap with landslide mapping grids containing Cyclone Gabrielle landslide data needed for model validation (Leith et al. 2023). As of 1 November 2023 only 19% of the region had been mapped (see Figure 1). This included 103,989 landslides of different movement types and materials. More than 86% of mapped landslides were soil or debris material, approximately 1% were rockfalls, and 6% contained woody debris. In terms of movement type, most landslides (98.2%) were slides or flows. For the purposes of this research, landslides classified as rockfalls were excluded from further analysis.

Additional preprocessing steps applied to the landslide inventory included the removal of scar (source area) duplicates and scars mapped without landslide deposits. Also, scar points located within the LiDAR-derived stream network (see section 4.4 for details) were considered stream bank failures and were excluded. Overall, 2.2% of mapped landslides were removed from the initial data set for the above-mentioned reasons.

The selection procedure produced 50 farm-pasture polygons for high-resolution modelling, with areas that ranged from 1 to 11.5 km^2 (2.9 km^2 median). The selected farm-pasture polygons span a large range of rainfall and landslide densities (cf. Appendix). On average, the farm-pasture polygons received 354 mm of rainfall, ranging from 253 mm for farm No. 21 to 519 mm for farm No. 39. Across all 50 farms a total of 20,392 landslides were triggered by Cyclone Gabrielle. Landslide densities ranged from 11 scars/km^2 (farm No. 42) to 300 scars/km^2 (farm No. 40), with an average of 113 scars/km^2. An average existing tree density on LCDB-mapped pastoral land was 695 trees/km² and ranged from 114 trees/km² to 2,201 trees/km².

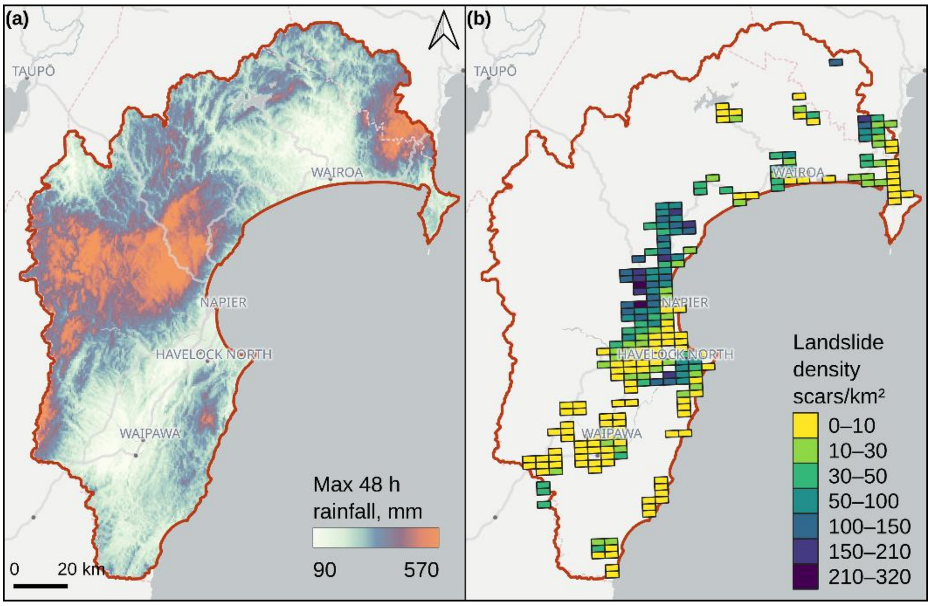

Figure 1. Hawke's Bay region overview: (a) maximum cumulative rainfall for 48 h during Cyclone Gabrielle (source: HBRC); (b) Cyclone Gabrielle landslide densities within mapping grids (source: GNS-led mapping project, Leith et al. 2023).

4.2 Tree influence model on slope stability (TIMSS)

We calibrated the statistical model representing the influence of individual trees on landslide susceptibility (Spiekermann et al. 2021, 2022a, 2022b, 2023) using available data on individual trees, landslide scar areas, and the LiDAR DEM for pastoral areas. The spatial data on individual trees was produced as part of the HBRC–MWLR LiDAR partnership project (2022–2024), where trees were delineated from the LiDAR-derived DEM and canopy height model using the PyCrown algorithm (Zörner et al. 2018). The minimum tree detection height and radius were 0.5 m.

The $TIMSS$ calibration required high-resolution landslide scar area (polygon) data to quantify the extent to which the area of landslide-eroded land was influenced by proximity to individual trees. For this we used landslide scar-mapping data from the March 2022 storm events in northern Hawke's Bay (Betts et al. 2023) and a multi-temporal landslide data set from Wairarapa (Spiekermann et al. 2021, 2022b), given that equivalent scar polygon data from high-resolution mapping are not available for Cyclone Gabrielle. This step improved the applicability of the original $TIMSS$ model to Hawke's Bay by using data from the region.

The $TIMSS$ represents the average influence of an individual tree on slope stability and has the following attributes (Spiekermann et al. 2023).

- Values are spatially distributed as a function of distance from the tree (trunk).
- Contributions of neighbouring trees to slope stability are considered additive.

- Local hydrological and mechanical effects are represented implicitly.

The original approach by Spiekermann et al. (2021) was developed for four different tree species (poplar, willow, kānuka, conifer, and eucalyptus). However, since no species data were available in the Hawke's Bay data set, we calibrated the model using a combined $TIMSS$ (i.e. one tree influence model on slope stability for all tree species). On the one hand, this approach does not allow for a detailed study of the impact of a specific tree type on slope stability (Spiekermann et al. 2022a); on the other hand, it enables calibration of $TIMSS$ with an increased number of tree data points (Spiekermann et al. 2021).

Combining the Wairarapa and northern Hawke's Bay data sets produced a database of 88,948 landslide scar polygons. To create the $TIMSS$, first we selected only those trees that stand at a distance of at least 15 m from other trees to isolate the influence of individual trees on slope stability for the purpose of model calibration (Spiekermann et al. 2021). Then we kept only those trees that were located on pastoral land by intersecting with LCDB v5.0 2018 'pasture' polygons (see section 4.1 for definition). In addition, trees were excluded if located on slopes where landslides were considered less likely to occur, defined as slopes below 17.5° (Spiekermann et al. 2021). This threefold selection procedure resulted in a data set comprising 160,429 individual trees.

Two final steps were involved in the calculation of the $TIMSS$. First, the landslide scar polygons were gridded at a 1 m resolution to create a binary grid of eroded soil surface and non-landslide eroded areas. Next, for each tree we calculated the number of landslide-eroded and stable (i.e. non-landslide) pixels within a radius from 0 to 40 m (r). Thus, for each tree we calculated the tree influence with a precision of 1 m, expressed as a fraction of eroded pixels of all land around the tree. The fraction of landslide eroded area as a function of distance from the tree $f(r)$ could then be calculated for the whole data set by aggregating by r.

A non-linear least-squares logistic regression model was used to fit $f(r)$. The logistic growth function was defined as:

$$f(r) = \frac{b_c}{1+e^{\frac{xmid-r}{scal}}} \tag{1}$$

where b_c is a parameter representing the asymptote; $xmid$ is a parameter representing the r value at the inflection point of the curve; and $scal$ is the scale parameter on the input axis. Thus, the $TIMMS$ was defined as the proportional reduction in landslide-eroded area, expressed as:

$$TIMSS = b_c - f(r) = 1 - \frac{1}{1+e^{\frac{xmid-r\prime}{scal}}} \tag{2}$$

where $TIMSS$ is the mitigation at a given pixel for an individual tree.

When applied spatially, the influence of more than one tree is assumed to be additive, and the upper limit on the number of trees contributing to slope stability at a given pixel is assumed to be four (Spiekermann et al. 2021). The $TIMSS$ was thus a two-dimensional representation of biophysical erosion and sediment control at 1 m resolution (see Figure 2).

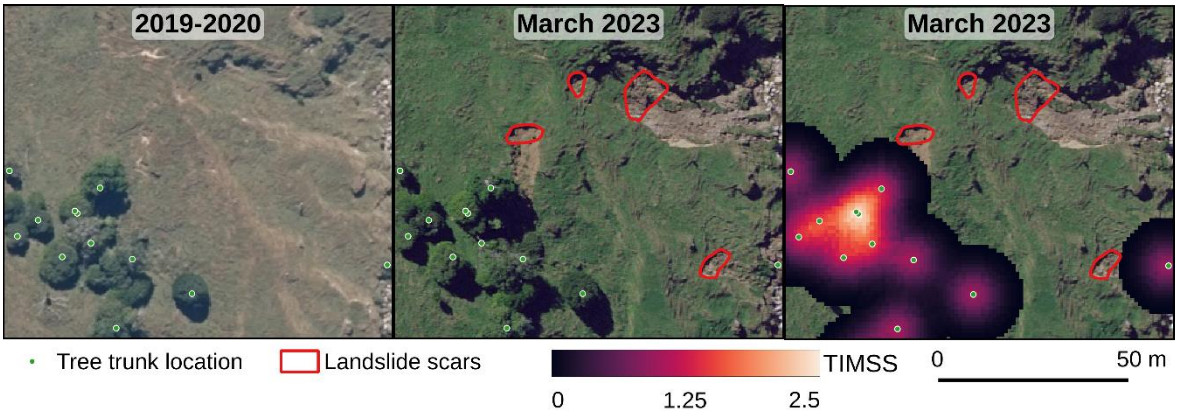

Figure 2. Illustration of spatial application of the $TIMSS$. Multiple landslides occurred during the Cyclone Gabrielle, which can be seen on March 2023 imagery, compared to previous one. Although trees contribute to slope stability, they do not always prevent landslide erosion – a reflection of a multivariate problem. Note that the influence of more than one tree at a given location is assumed to be additive, which is why values exceed 1.

The results of the $TIMSS$ recalibration are shown in Figure 3. The points in Figure 3(a) are the measured mean values of fractions of eroded soil at each 1 m increment away from individual trees. Figure 3(b) shows the results of the normalised reduction in eroded soil (eq. 2). Where the layout of trees is such that more than one tree contributes to slope stability at a given location, the influence on slope stability is assumed to be additive. Therefore, $TIMSS$ values can exceed 1 when applied spatially (see Figure 2). The normalised tree influence on slope stability decreased rapidly with increasing r, dropping to 0.5 at 6 m (Figure 3(b)). The maximum effective distance was 13 m.

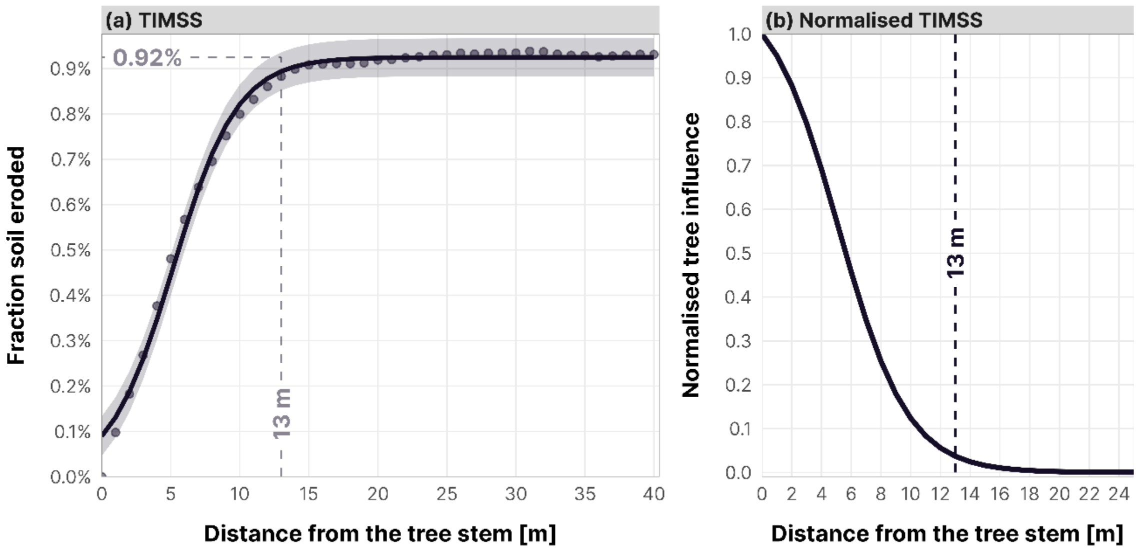

Figure 3. (a): Mean fraction of eroded soil by distance from tree, fitted using a non-linear logistic regression model with a 95% confidence band. (b): normalised mean tree influence for an individual tree, as a reduction in eroded soil. Vertical lines show the maximum effective distance of 13 m.

4.3 Landslide susceptibility modelling

The $TIMSS$-based landslide susceptibility model was applied following the method described in Spiekermann et al. 2022b using a combined shallow landslide inventory based on mapping from high-resolution imagery in northern Hawke's Bay and Wairarapa (Spiekermann et al. 2021; Betts et al. 2023). The inventory consisted of *ca.* 58,000 rainfall-induced shallow landslides on pastoral land. Binary logistic regression (BLR) is frequently used for statistical landslide susceptibility modelling because it represents the probability of a binary response variable, which corresponds to the absence or presence of landslides (Smith et al., 2023). We used a 1:1 balanced sample design, with an equal number of landslide presence and randomly generated landslide absence points.

To develop the statistical model of landslide susceptibility, key predictor variables of shallow landslide erosion were generated from existing terrain and lithology data sets. The initial selection of predictor variables was based on a geomorphological understanding of physical processes that might influence slope stability, supported by the findings of recent studies of landslide susceptibility in New Zealand (Spiekermann et al. 2022; Smith et al. 2023). Therefore we included: the topographic variables of slope, gradient and aspect (northernness, easternness); tree cover using $TIMSS$; and top rock lithology from the New Zealand Land Resources Inventory (Newsome et al. 2008). BLR modelling was performed using the tidymodels framework (Kuhn & Wickham 2020), and the terra package (Hijmans 2023) was used for spatial model predictions, both of them within the open-source statistical software R 4.4.0 (R Core Team 2024).

To test model prediction performance, we used k-fold ($k = 10$) cross-validation (CV). Samples were randomly partitioned into 10 folds, whereby 9 folds were used to train the model and the remaining fold used to test the predictive ability of the model using selected performance metrics. This procedure was repeated until each of the 10 folds had been used for model testing. To ensure the performance measures were not influenced by a particular data partitioning, this process was repeated five times. Moreover, we used 100 balanced bootstraps (with an equal number of absence and landslide points), each with a different set of randomly selected absence points for the five repeats of k-fold CV.

Model classification performance was evaluated using receiver operating characteristic curves and calculation of the area under the receiver operating characteristic curve ($AUROC$) using the yardstick R-package (Kuhn et al. 2023). A good $AUROC$ score is considered to be between 0.8 and 0.9, while an excellent score is greater than 0.9 (Obuchowski 2003). We also estimated an F_1 score, which is a confusion matrix metric widely used in the binary classification of balanced data sets (Chicco & Jurman 2020). The F_1 is defined as the harmonic mean of precision and recall:

$$F_1 = \frac{2 \times TP}{2 \times TP + FP + FN}, \quad (3)$$

where true positives (TP) are the correct predictions, while false negatives (FN) and false positives (FP) are the incorrect predictions. The F_1 ranges from 0 to 1, where $F_1 = 1$ corresponds to perfect classification. Usually, classification with an F_1 score higher than 0.7 is considered 'good' (Chicco & Jurman 2020).

The model that corresponded to the median $AUROC$ value of 0.91 and F_1 of 0.85 was selected and used for spatial prediction. We classified the spatial probabilities of the landslide susceptibility map into three classes based on thresholds related to the percentage of observed landslides falling within each susceptibility class. Class thresholds were determined by ranking the landslides used to fit the model by their probability values in decreasing order (Spiekermann et al. 2022). The 'high' class contains 80% of the mapped landslides, which have probabilities ≥ 0.60, while the 'moderate' class corresponds to a further 15% of landslides (probabilities ≥ 0.38 to <0.60), and the remaining 5% of landslides fall into the class 'low' (probabilities < 0.38).

4.4 Landslide-to-stream connectivity modelling

Morphometric landslide-to-stream connectivity was trained based on a LiDAR-derived 5 m DEM using a binary logistic regression model (Spiekermann et al. 2022a; Tsyplenkov et al. 2023). Connectivity was expressed as a spatial probability (range 0–1), where areas with values close to 1 have a higher likelihood of connecting to a stream network, while areas close to zero have a low likelihood of connection. The DEM-derived stream network (using a D8 flow accumulation algorithm and a 10 ha channel initiation threshold; refer to Smith et al. 2024) was merged with a derived national layer comprising river and lake polygons, which was used to represent wide river channels and waterbodies (Smith & Betts 2021).

The BLR model was fitted using spatial covariate data for connected and disconnected landslide source areas (mapped with centroid points), obtained from mapping areas that intersect with available LiDAR coverages in the Hawke's Bay, Gisborne, and Greater Wellington regions. The combined landslide source and deposit inventory presently comprises approximately 41,000 landslides, where 8.5% of them are connected to the stream network. Our results revealed a strong dependency of connectivity on the overland flow distance to the stream network ($DownDist$). Results obtained from this single-variable model exhibited similar predictive performance compared to more complex, multi-variable models (Tsyplenkov et al. 2023).

We cross-validated the BLR model within the tidymodels R-package infrastructure (Kuhn & Wickham 2020) using the following procedure.

1 Balanced bootstrap resampling was performed with replacement, ensuring that every bootstrap had an equal amount of connected and disconnected landslides.

2 Each bootstrap resample was further split into training and testing data sets, and the model was fitted to the training data set.

3 The testing data set was used to evaluate the model performance with a set of metrics described in section 4.3.

The whole procedure was repeated and produced 100 different models, with their corresponding parameter estimates and model metrics. The model with the highest $AUROC$ value was used for predictions. In the present version, the BLR model achieved a median $AUROC$ of 0.87 in cross-validation.

We classified spatial probabilities predicted with the BLR model into three classes (high, moderate, and low). As with the landslide susceptibility classes, the thresholds used to define each connectivity class were determined by ranking the connected landslides used to fit the model by their probability values in decreasing order. 'High' connectivity corresponds to 80% of the mapped landslides, which have probability values ≥ 0.58. 'Moderate' corresponds to a further 15% of the mapped landslides, which have probability values between ≥0.18 to <0.58, while 'low' relates to the remaining 5% of landslides, with values < 0.18.

We also estimated the class-specific sediment delivery ratio (SDR, dimensionless) based on Cyclone Gabrielle landslide mapping. In the absence of data on landslide-eroded volumes or areas for estimating SDRs, it was necessary to rely on count data using point-based landslide mapping (Leith et al. 2023). SDR_{ij} describes the proportion of all mobilised material entering the stream network for the ith connectivity class and jth farm. SDR_{ij} was calculated for each connectivity class i (high, moderate, and low) based on the estimated volume of connected scars from class i (LCV_{ij}) per farm j relative to the total estimated landslide scar volume in class i per farm j (LV_{ij}), following Spiekermann et al. (2022a).

$$SDR_{ij} = \frac{LCV_{ij}}{LV_{ij}} \times DR \tag{4}$$

To compute SDRs, we assumed that shallow landslides had a mean depth of 1 m based on studies reporting shallow landslide depths in hill country terrain (Crozier 1996; Reid & Page 2003; Betts et al. 2017). Data on landslide source areas were unavailable, so we used the median landslide area from landslide polygon mapping across northern Hawke's Bay following the March 2022 storm events (Betts et al. 2023). The median landslide scar area was 89 m^2 based on 35,710 landslides mapped within pastoral areas. The delivery rate (DR) was set to 0.5 for the stream network, which indicates that, on average, connected landslides deliver approximately 50% of mobilised sediment to the stream (Reid & Page 2003; Spiekermann et al. 2022a).

4.5 Coupling landslide susceptibility and connectivity

We integrated spatial predictions of landslide susceptibility and connectivity. First, we reclassified the continuous susceptibility and connectivity probability rasters into classes using thresholds described above. An intersection of the two reclassified spatial predictions resulted in an initial matrix of nine joint classes describing both the likelihood of landslides occurring in the future and the potential for sediment to be delivered to the stream network. We named the classes accordingly (i.e. the intersection of high susceptibility and high connectivity classes produced 'High LS / High Con' corresponding to a class where landslides are likely to occur and reach the stream network). To avoid ambiguous situations where high connectivity exists while the landslide susceptibility is low, we merged all connectivity classes in the low susceptibility zone into one, referred to as 'Low LS' (see Figure 4).

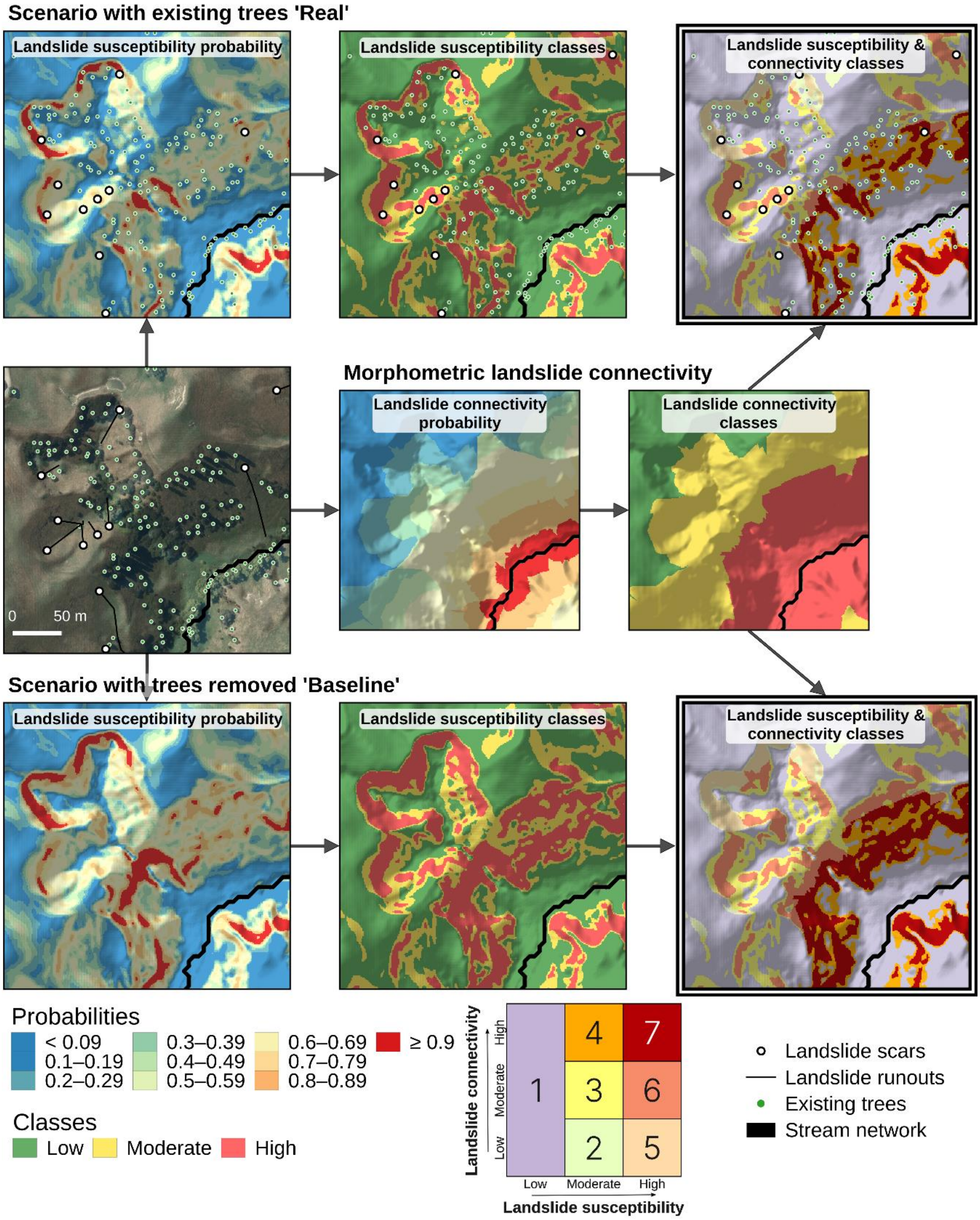

Figure 4. Scheme illustrating the integration of class-based shallow landslide susceptibility and connectivity model outputs for two scenarios: 'baseline' with trees removed and 'real' with existing trees.

4.6 Effectiveness of trees on farms

Based on the $TIMSS$ calibration described in section 4.2, landslide susceptibility modelling was performed for farms selected in section 4.1. This produced estimates of the influence of existing trees in pastoral areas on landslide susceptibility at 1 m resolution ('real' scenario). For comparison, the existing trees were removed from pastoral areas, and landslide susceptibility was estimated for a treeless reference condition ('baseline' scenario). The difference between these two layers (existing trees vs treeless reference) provided the basis for quantifying the influence of existing trees on landslide susceptibility at the farm scale. This difference is expressed in terms of a change in the number of landslides (N) per farm, based on the mapped landslide spatial density (scars/km^2) corresponding to different susceptibility classes, and the change in sediment delivery to streams (SY) per farm.

4.7 Farm-scale landslide sediment delivery to streams

We estimated the average reduction in sediment load delivered to the stream network that can be attributed to the presence of individual trees in pastoral areas for the selected farms during Cyclone Gabrielle. Combining tree-level susceptibility modelling (section 4.3) and a morphometric landslide connectivity model (section 4.4) allowed us to estimate how the presence of individual trees influences both landslide susceptibility and connectivity at the farm scale.

Reductions in shallow landslide erosion and sediment delivery were based on estimated changes in event sediment yield (SY, t/km^2) between the baseline and real scenarios. To estimate the reduction in landslide sediment yield per farm, we used the Cyclone Gabrielle landslide density per joint susceptibility and connectivity class (described in section 4.5) per farm to estimate the total number of landslides per farm, based on the change in joint class area following the removal of trees in the baseline scenario. The total number of landslides per farm under the baseline scenario was estimated by multiplying the class-specific landslide densities by the class areas for each farm.

The median landslide area (A, 89 m^2) and a landslide depth (D, 1 m) derived from earlier work in the absence of data from Cyclone Gabrielle were used to estimate the farm-specific event sediment yield (SY_j) for both scenarios (i.e. SY_{baseline} and SY_{real}):

$$SY_j = \frac{\sum_{n=1}^{i} SDR_{ij} \times N_{ij} \times A \times D \times \rho}{P_{\mathrm{j}}}, \tag{5}$$

where P_{j} is the pastoral area for the jth farm (km^2); SDR_{ij} and N_{ij} are the sediment delivery ratio and landslide number (respectively) for every joint class i and farm j (see section 4.5); and ρ is soil bulk density, equal to 1.4 t/m^3 (Spiekermann et al. 2022). The reduction in landslide sediment yield ($SY_{\text{reduction}}$, %) for the event was estimated as:

$$SY_{\text{reduction}} = 100 \times \frac{SY_{\text{real}} - SY_{\text{baseline}}}{SY_{\text{baseline}}} \tag{6}$$

5 Results

5.1 Landslide susceptibility and connectivity

The interim landslide mapping data available for Cyclone Gabrielle in the Hawke's Bay region (Leith et al. 2023) was not used in training the susceptibility and connectivity models, which means these data provide a basis for independently assessing the class-based susceptibility and connectivity maps (see Figure 4). We found that most (63%) Gabrielle-triggered shallow landslides occurred in the high susceptibility class, while 24% occurred in the moderate class, and 13% in low.

The proportion of Gabrielle-triggered landslides connected to streams with source areas (mapped using points) located in the high connectivity class area equated to 54%, while 25% of the connected landslides occurred in the moderate class and 21% in the low class. The farm average proportion of connected landslides in the high connectivity class was 67%, moderate was 18%, and low was 15%.

The median estimated SDR value for the high connectivity class was 0.14, for moderate it was 0.04, and for low it was 0.01, based on the Gabrielle landslide mapping data for each farm (Figure 5). The highest SDR values were observed at those farms where most landslides were triggered in the high connectivity class and landslide runout reached the stream network. For example, at farm No. 7, 39 out of 57 landslides in the high connectivity class were connected to streams. In contrast, the lowest SDR values were observed at farms where there were no connected landslides mapped; for example, at farm No. 11 none of the 84 mapped landslides reached the stream network.

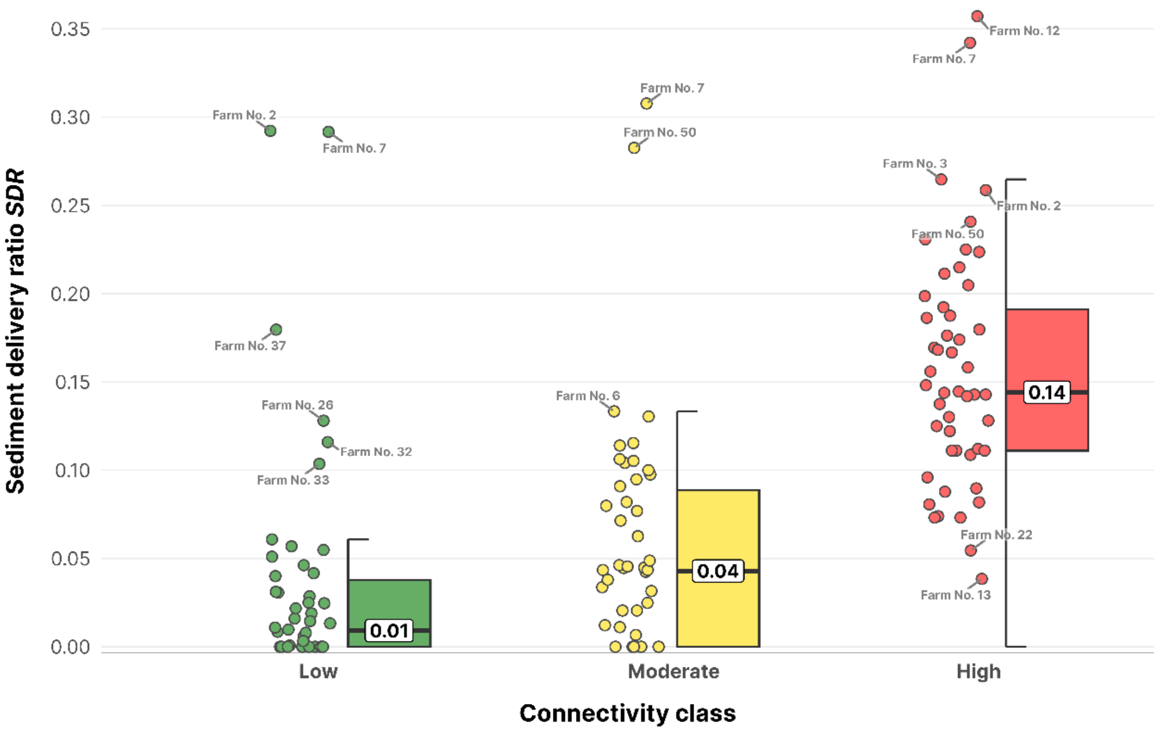

Figure 5. Distributions of estimated farm and class-specific SDRs based on the Cyclone Gabrielle landslide mapping data (Leith et al. 2023). SDR was estimated according to Equation 4, with the 10 ha digital stream network as the connectivity target.

5.2 Farm-scale landslide sediment delivery

Cyclone Gabrielle triggered 20,392 shallow landslides across all the selected farms. The corresponding gross landslide erosion was estimated to be 2.54 × 10^6 t, while an estimated 0.17 × 10^6 t of landslide-derived sediment reached the stream network. Across the selected farms, on average 7.5% of eroded material reached the stream network, ranging from 0 to 32%.

The estimated farm-scale sediment yield delivered to the stream network from shallow landslides ranged from 0 to 3,707 t/km², with a median of 723 t/km² for the real scenario (Figure 6). The highest SY_{real} was observed at farm No. 6, where 314 landslides were mapped and the corresponding SY_{real} was 3,707 t/km². The lowest SY_{real} was observed at farm No. 11, with 84 landslides mapped and an SY_{real} of 0 t/km², since no landslides were connected to the stream network (Table 1).

With trees removed from pastoral areas (i.e. the baseline scenario), we estimated that 22,257 shallow landslides (8.4% more) could have been triggered by Cyclone Gabrielle across the modelled farms. That count resulted in gross landslide erosion of 2.77 × 10^6 t with an estimated 0.18 × 10^6 t delivered to the stream network. The increase in landslides corresponds to a farm $SY_{baseline}$ delivered to the stream network ranging from 0 to 4,173 t/km², with a median of 813 t/km².

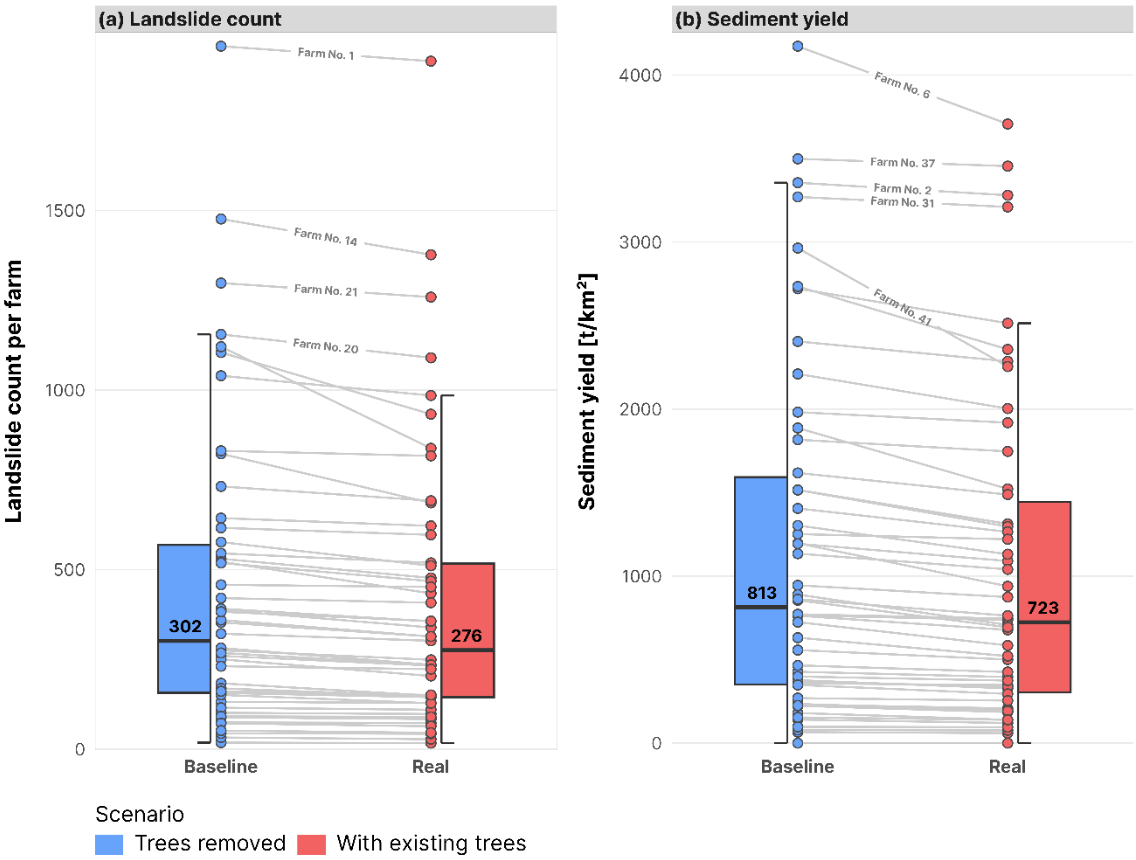

Figure 6. Estimated reduction in landslide number (a) and sediment yield (b) across the selected farms between the two scenarios: baseline with trees removed and real with existing trees.

Table 1. Summary of the two modelled scenarios: baseline (with trees removed) and real (with existing trees) across the 50 selected farms, expressed as landslide number per farm, landslide spatial density per farm, landslide sediment yield delivered to the stream network per farm, and estimated proportional reduction in landslide number and sediment yield, based on comparison of the baseline and real scenarios.

HBFID	Landslide number per farm		Landslide density per farm (scars/km^2)		Landslide sediment yield per farm (t/km^2)		Reduction (%)	
	Baseline	Real	Baseline	Real	Baseline	Real	Landslide number	Sediment Yield
41	1,121	838	372	278	2,964	2,255	25	24
23	184	149	82	67	180	140	19	22
44	282	235	224	186	1,197	939	17	22
40	823	686	359	300	889	708	17	20
35	522	434	143	119	1,887	1,522	17	19
19	577	511	129	114	724	585	11	19
24	1,105	933	300	253	855	694	16	19
27	360	314	100	88	632	521	13	17
30	260	233	97	87	223	186	10	17
15	250	204	88	71	235	196	19	16
45	151	128	143	121	348	295	15	15
49	52	46	40	35	225	192	11	15
43	33	28	32	27	141	121	14	14
34	387	339	122	107	1,516	1,297	13	14
32	268	235	225	198	2,735	2,358	12	14
18	530	477	140	126	1,516	1,313	10	13
50	72	64	50	45	1,303	1,131	11	13
12	18	17	16	15	377	328	7.4	13
36	519	468	96	87	862	763	9.7	11

HBFID	Landslide number per farm		Landslide density per farm (scars/km^2)		Landslide sediment yield per farm (t/km^2)		Reduction (%)	
	Baseline	Real	Baseline	Real	Baseline	Real	Landslide number	Sediment Yield
6	353	314	212	189	4,173	3,707	11	11
25	276	249	81	73	763	678	9.6	11
3	158	151	45	43	557	501	4.4	10
26	161	145	96	87	1,406	1,265	10	10
39	169	148	94	82	231	208	13	9.8
13	322	302	51	48	66	60	6.1	9.8
28	391	356	188	171	2,211	2,004	9	9.4
48	161	151	36	34	154	140	6.4	9.3
5	732	692	160	151	1,194	1,091	5.4	8.7
14	1,477	1,377	153	143	465	426	6.7	8.5
17	383	357	133	124	1,135	1,041	6.7	8.3
20	1,155	1,090	216	203	1,618	1,488	5.7	8
22	115	110	105	100	368	338	4.7	8
7	157	145	69	64	2,721	2,514	7.5	7.6
10	1,040	985	135	128	945	874	5.3	7.5
8	101	98	59	57	427	396	3.3	7.3
16	158	151	106	101	399	374	4.6	6.1
46	231	223	33	31	270	255	3.5	5.5
33	545	519	182	173	2,405	2,286	4.8	4.9
9	421	408	148	143	1,817	1,747	3.1	3.9
21	1,298	1,259	169	164	765	738	3	3.5
29	644	622	107	103	771	746	3.3	3.3

HBFID	Landslide number per farm		Landslide density per farm (scars/km²)		Landslide sediment yield per farm (t/km²)		Reduction (%)	
	Baseline	Real	Baseline	Real	Baseline	Real	Landslide number	Sediment Yield
38	616	597	144	139	1,982	1,919	3.2	3.2
4	74	73	52	51	358	347	2	3
1	1,958	1,916	170	166	1,252	1,221	2.1	2.4
42	44	43	11	11	79	77	2.7	2.4
2	132	129	105	103	3,356	3,281	2.3	2.2
47	91	90	28	28	97	95	1.6	2.1
31	831	817	207	203	3,271	3,211	1.7	1.8
37	458	452	168	166	3,499	3,455	1.3	1.3
11	89	84	44	41	—*	—*	5.3	—*

* None of the mapped landslides on farm No. 11 reached the stream network during Cyclone Gabrielle; therefore, the sediment yield for both scenarios has not been estimated.

5.3 Effectiveness of trees on farms

Our modelling across the 50 farms showed that, under the treeless baseline scenario, only 5.7% (9.6 km^2) of the total pastoral area on the farms is both highly susceptible to shallow landsliding and has high potential for sediment delivery to the stream network (i.e., 'High LS / High Con'). However, due to the actual tree cover (real scenario), this class is reduced to 4.7% of the total area. The class reduction resulted in the prevention of an additional 1,865 landslides occurring (8.4%), or, when expressed as gross landslide erosion, 0.23×10^6 t of eroded material.

The existing tree cover on pastoral land led to an estimated 9% reduction in landslide sediment delivery to streams when summed across all farms. This proportional reduction equates to approximately 16,150 t of sediment that was prevented from reaching the stream network due to the influence of trees in stabilising land and reducing the occurrence of landslides during Cyclone Gabrielle.

The presence of trees in pastoral areas achieved a median 7% estimated reduction in landslide numbers across the 50 farms. When expressed as SY, this equated to a median 10% decrease (Figure 7). Based on the individual farm results, we can see that the presence of trees produced up to a 24% reduction in landslide sediment delivery to the stream network. This result was achieved where trees occurred in areas that were highly susceptible and where landslides were highly likely to connect to the stream network (i.e. steep slopes proximal to the stream network).

At farms with an SY reduction greater than or equal to 15%, the individual tree density (defined as trees that stand at least 13 m from other trees, see Figure 3) ranged from 145 to 241 trees/km^2, with an average of 193 trees/km^2. For farms with a lower observed reduction (<5%), the average individual tree density was 85 trees/km^2, ranging from 32 to 160 trees/km^2.

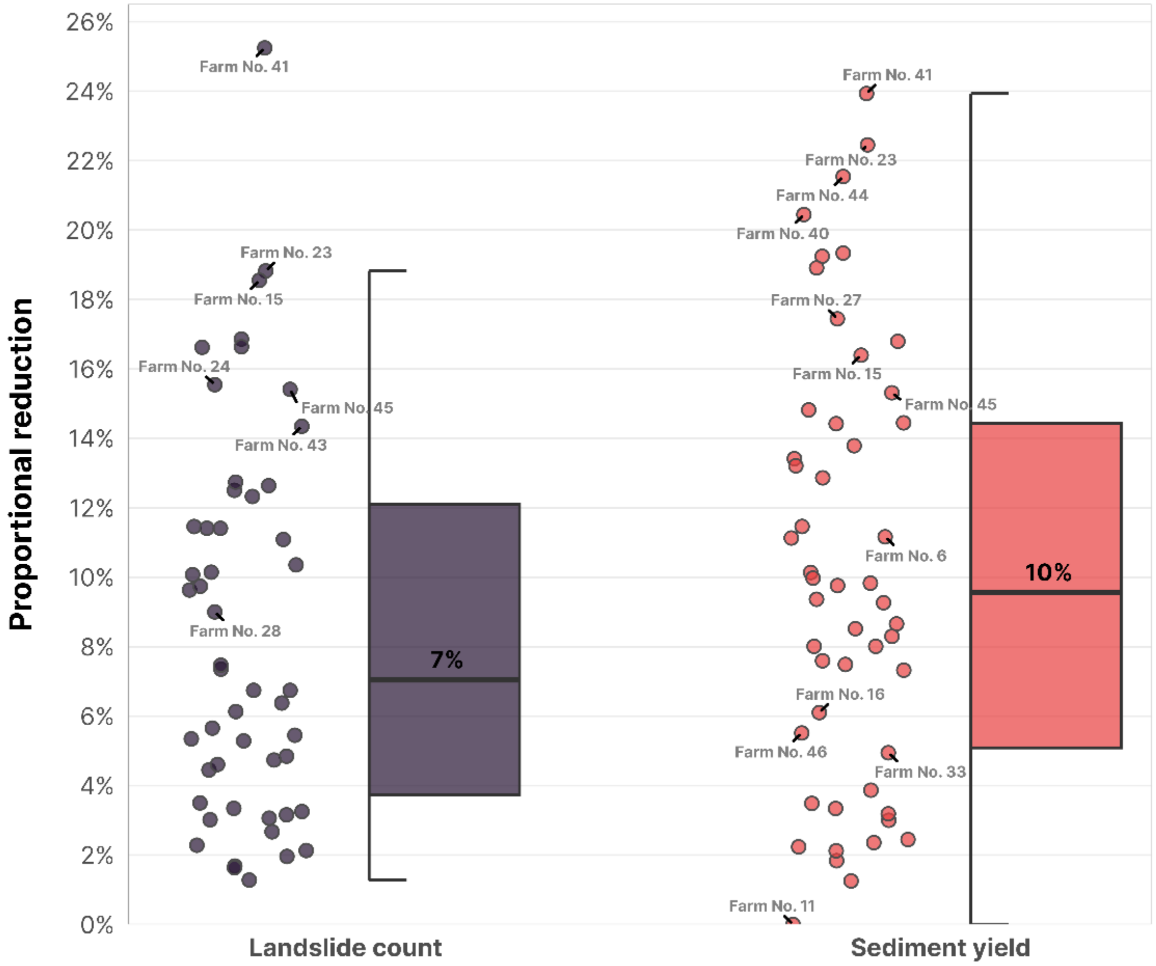

Figure 7. Proportional reduction (%) in landslide number and sediment yield delivered to the stream network across the selected farms in the two scenarios: baseline, with trees removed, and real, with existing trees.

Pearson r correlation analysis showed a moderate (r = 0.51) but statistically significant (p < 0.001) positive correlation between the estimated maximum 48 h rainfall during Cyclone Gabrielle and farm-scale landslide density. That provides evidence that more landslides were triggered with increasing rainfall intensity, which is consistent with previous findings (e.g. Smith et al. 2023).

Our analysis revealed that it is not only the number of trees located in areas highly susceptible to landslide occurrence that might influence sediment delivery to streams, but also the location of those highly susceptible zones within a farm. The pastoral hillslopes of farm No. 49 (Figure 8) illustrate this. According to our estimation, SY reduced from 225 t/km^2 in the baseline scenario to 192 t/km^2 in the real scenario. This 15% reduction in yield was largely achieved because trees in pastoral areas on this farm occur in proximity to the stream network. Moreover, the presence of trees in pastoral areas of this farm produced a 24% reduction in the 'High LS / High Con' class area.

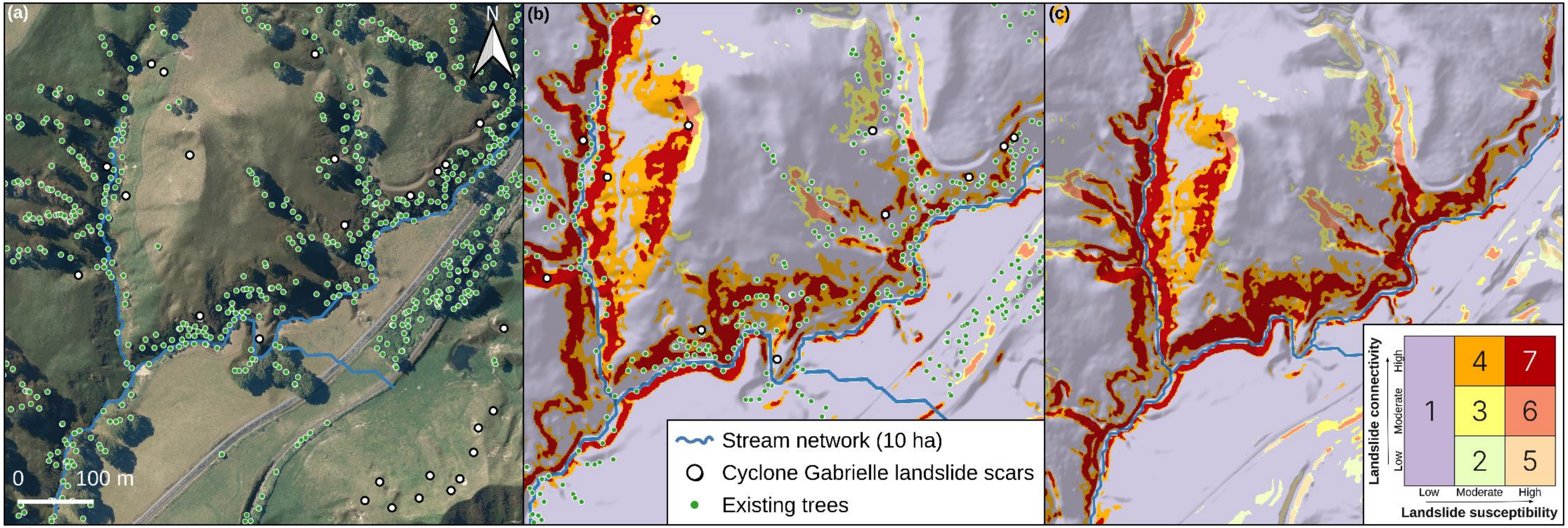

Figure 8. The influence of individual trees on the spatial extent of areas highly susceptible to landslide occurrence and connectivity to streams: (a) satellite imagery of farm No. 49, showing the location of existing trees and mapped landslide scars after Cyclone Gabrielle (landslide data from Leith et al. 2023); (b) modelled shallow landslide susceptibility and connectivity for the real scenario (i.e. with existing trees); (c) modelled shallow landslide susceptibility and connectivity for the baseline scenario (i.e. with trees removed). Note the reduction in 'High LS / High Con' areas from (c) to (b).

6 Conclusions and recommendations

The present report estimates the magnitude of reductions in the number of shallow landslides and landslide sediment delivered to streams that may have been achieved by the presence of individual trees on pastoral areas in the Hawkes Bay region during Cyclone Gabrielle. We focused on 50 farms that experienced high rainfall but variable levels of landsliding, and modelled two scenarios: baseline, with all existing trees removed, and real, with existing tree cover.

Our analysis revealed that existing tree cover prevented the additional occurrence of 1,865 landslides (or 0.23×10^6 t of eroded material) across all modelled farms, with a median farm-scale reduction in landslide count of 7%. When expressed as a sediment yield delivered to the stream network, the reduction equates to a median 10% decrease. Where trees were located in close proximity to the stream network and on susceptible slopes, farm-scale reductions in sediment delivery to streams of up to 24% were estimated. Our modelling suggested that existing tree cover prevented approximately 16,150 t of landslide-derived sediment from reaching the stream network during Cyclone Gabrielle across the selected farms.

We found that the main driver of the reductions in sediment delivery was tree density in pastoral areas highly susceptible to landslides where landslide runout was likely to connect with the stream network. Due to the presence of existing trees, this area has already been reduced from 5.7% to 4.7% across the selected farms. Further reductions in future landslide sediment delivery to streams may be achieved through additional tree planting targeting pasture areas that are highly susceptible and highly likely to produce landslides that connect to streams. These areas have been identified in the farm-scale landslide susceptibility and connectivity maps accompanying this report.

Future applications of the $TIMSS$-based landslide susceptibility and connectivity model framework could extend to a larger number of farms and focus on estimating reductions in landslide sediment delivery to streams that might be achieved using targeted approaches to tree planting. This could include testing scenarios involving different tree densities or planting patterns, including the targeted planting of spaced trees to pasture areas based on the high-resolution landslide susceptibility and connectivity maps.

7 Acknowledgements

This work was funded by the New Zealand Ministry of Business, Innovation & Employment (MBIE) through the Extreme Weather Recovery Advice Fund (contract ID C09X2303). We acknowledge staff from Hawke's Bay Regional Council, particularly Ashton Eaves and Kathleen Kozyniak, for discussions leading to this work and for the provision of spatial data. We are grateful to GNS Science for early access to the Cyclone Gabrielle landslide inventory. We thank Andrew Neverman for reviewing the report.

8 References

Basher L, Spiekermann R, Dymond J, Herzig A, Hayman E, Ausseil A-G 2020. Modelling the effect of land management interventions and climate change on sediment loads in the Manawatu-Whanganui region. New Zealand Journal of Marine and Freshwater Research 54: 490–511.

Betts H, Basher L, Dymond J, Herzig A, Marden M, Phillips C 2017. Development of a landslide component for a sediment budget model. Environmental Modelling & Software 92: 28–39. https://doi.org/10.1016/j.envsoft.2017.02.003

Betts H, Smith HG, Neverman AJ, Tsyplenkov A 2023. Wairoa shallow landslide and debris deposit mapping following storm events in March 2022. Manaaki Whenua – Landcare Research contract report LC4331 for Hawke's Bay Regional Council.

Chicco D, Jurman G 2020. The advantages of the Matthews correlation coefficient (MCC) over F1 score and accuracy in binary classification evaluation. BMC Genomics 21(1): 6. https://doi.org/10.1186/s12864-019-6413-7

Crozier M 1996. Runout behaviour of shallow, rapid earthflows. Zeitschrift Für Geomorphologie. Supplementband 105: 35–48.

Hijmans RJ 2023. terra: Spatial data analysis. https://CRAN.R-project.org/package=terra

Kuhn M, Vaughan D, Hvitfeldt E 2023. yardstick: Tidy characterizations of model performance. https://CRAN.R-project.org/package=yardstick

Kuhn M, Wickham H 2020. Tidymodels: a collection of packages for modelling and machine learning using tidyverse principles. https://www.tidymodels.org

Leith K, McColl S, Robinson T, Massey C, Townsend D, Rosser B, et al. 2023. Reflections on the challenges of mapping >100,000 landslides triggered by Cyclone Gabrielle. Geoscience Society of New Zealand Annual Conference 2023, Abstracts 164A, 280.

Newsome PFJ, Wilde RH, Willoughby EJ. 2008. Land Resource Information System Spatial Data Layers: Data Dictionary. Landcare Research New Zealand Ltd, Palmerston North. http://digitallibrary.landcareresearch.co.nz/cdm/ref/collection/ p20022coll14/id/67.

Obuchowski NA 2003. Receiver operating characteristic curves and their use in radiology. Radiology 229(1): 3–8. https://doi.org/10.1148/radiol.2291010898

R Core Team 2024. R: a language and environment for statistical computing. Vienna, R Foundation for Statistical Computing. https://www.R-project.org/

Reid LM, Page MJ 2003. Magnitude and frequency of landsliding in a large New Zealand catchment. Geomorphology 49(1–2): 71–88. https://doi.org/10.1016/S0169-555X(02)00164-2

Sanson RL 2005. The AgriBase farm location database. Proceedings of the New Zealand Society of Animal Production 65: 93–96.

Smith HG, Betts H 2021. Memorandum on implementing a national index for susceptibility to streambank erosion. Manaaki Whenua – Landcare Research contract report LC3998 for the Ministry for the Environment.

Smith HG, Neverman AJ, Betts H, Herzig A 2024. Improving understanding and management of erosion with LiDAR. Manaaki Whenua – Landcare Research contract report for Hawke's Bay Regional Council.

Smith HG, Neverman AJ, Betts H, Spiekermann R 2023. The influence of spatial patterns in rainfall on shallow landslides. Geomorphology 437: 108795. https://doi.org/10.1016/j.geomorph.2023.108795

Spiekermann R, McColl S, Fuller I, Dymond J, Burkitt L, Smith HG 2021. Quantifying the influence of individual trees on slope stability at landscape scale. Journal of Environmental Management 286: 112194. https://doi.org/10.1016/j.jenvman.2021.112194

Spiekermann R, Smith HG, McColl S, Burkitt L, Fuller I 2022a. Development of a morphometric connectivity model to mitigate sediment derived from storm-driven shallow landslides. Ecological Engineering 180: 106676. https://doi.org/10.1016/j.ecoleng.2022.106676

Spiekermann RI, Smith HG, McColl S, Burkitt L, Fuller I 2022b. Quantifying effectiveness of trees for landslide erosion control. Geomorphology 396: 107993. https://doi.org/10.1016/j.geomorph.2021.107993

Spiekermann RI, van Zadelhoff F, Schindler J, Smith HG, Phillips C, Schwarz M 2023. Comparing physical and statistical landslide susceptibility models at the scale of individual trees. Geomorphology 440: 108870. https://doi.org/10.1016/j.geomorph.2023.108870

Tsyplenkov A, Smith HG, Betts H, Neverman AJ 2023. Data-driven shallow landslide connectivity analysis to reduce sediment delivery to streams. Geoscience Society of New Zealand Annual Conference 2023: Abstracts 164A, 280.

Zörner J, Dymond J, Shepherd J, Wiser S, Jolly B 2018. LiDAR-based regional inventory of tall trees – Wellington, New Zealand. Forests 9(11): 1–16. https://doi.org/10.3390/f9110702

Appendix – Summary statistics of pastoral areas within the 50 farms selected for further analysis.

HBFID	Farm-pasture area (km^2)	Mean 48 h rainfall during Cyclone Gabrielle (mm)	Fraction of farm area mapped by Leith et al. (2023)	Number of landslides	Landslide density ($scars/km^2$)	Spaced tree density ($trees/km^2$)
1	12	257	100%	1,916	166	47
2	1.2	347	100%	129	103	58
3	3.5	337	100%	151	43	56
4	1.4	336	100%	73	51	47
5	4.6	364	100%	692	151	74
6	1.7	407	100%	314	189	115
7	2.3	382	100%	145	64	116
8	1.7	322	100%	98	57	68
9	2.9	331	100%	408	143	88
10	7.7	302	100%	985	128	94
11	2	325	100%	84	41	74
12	1.1	321	100%	17	15	35
13	6.3	351	100%	302	48	92
14	9.7	278	100%	1,377	143	159
15	2.9	269	100%	204	71	99
16	1.5	348	100%	151	101	91
17	2.9	421	99%	357	124	196
18	3.8	349	100%	477	126	170
19	4.5	357	100%	511	114	152
20	5.4	416	99%	1,090	203	119
21	7.7	253	100%	1,259	164	82
22	1.1	290	100%	110	100	62
23	2.2	427	97%	149	67	143
24	3.7	496	100%	933	253	159
25	3.4	329	100%	249	73	162
26	1.7	320	100%	145	87	86
27	3.6	368	100%	314	88	97
28	2.1	425	100%	356	171	201
29	6	279	100%	622	103	153
30	2.7	373	100%	233	87	161
31	4	333	97%	817	203	95
32	1.2	436	100%	235	198	354
33	3	352	100%	519	173	162

HBFID	Farm-pasture area (km^2)	Mean 48 h rainfall during Cyclone Gabrielle (mm)	Fraction of farm area mapped by Leith et al. (2023)	Number of landslides	Landslide density ($scars/km^2$)	Spaced tree density ($trees/km^2$)
34	3.2	387	100%	339	107	174
35	3.6	289	96%	434	119	164
36	5.4	347	99%	468	87	194
37	2.7	431	100%	452	166	95
38	4.3	452	100%	597	139	115
39	1.8	519	100%	148	82	113
40	2.3	457	100%	686	300	243
41	3	480	100%	838	278	176
42	4.1	296	98%	43	11	29
43	1	364	100%	28	27	119
44	1.3	386	100%	235	186	211
45	1.1	342	100%	128	121	148
46	7.1	349	98%	223	31	145
47	3.3	270	98%	90	28	40
48	4.5	275	100%	151	34	99
49	1.3	270	100%	46	35	133
50	1.4	275	100%	64	45	112